Solid-State Electronics 208 (2023) 108730

Contents lists available at ScienceDirect

Solid State Electronics

journal homepage: www.elsevier.com/locate/sse

Monte Carlo study of electron–electron scattering effects in FET channels ☆

Josef Gull *, Hans Kosina

Institute for Microelectronics, TU Wien, Gußhausstraße 27–29, 1040 Wien, Austria

ARTICLE INFO

Keywords:
Electron–electron scattering
Monte-Carlo
Electronic transport
Energy distribution function

ABSTRACT

In this work, we study the effect of electron–electron scattering on the high-energy tail of the electron distribution function in FET channels. A new Monte Carlo algorithm for solving a two-particle kinetic equation in the presence of a position-dependent electric field is proposed. In stationary bulk simulations, no visible effect of electron–electron scattering on the distribution function and consequently on its moments is observed. In stationary device simulations, however, a clear effect on the high-energy tail can be seen. The enhancement of the tail relative to the thermal tail is found to scale with the electron concentration.

1. Introduction

Accurate knowledge about the energy distribution function (EDF) is essential to model the formation of hot carrier damage in semiconductor devices [1]. Electron–electron scattering (EES) can substantially impact the EDF [2–4] and has to be properly included in the transport model. Solution methods for the Boltzmann equation which becomes nonlinear in the presence of EES are either based on deterministic iterative methods [2] or ensemble Monte Carlo methods [5–7]. In this work we resort to a two-particle kinetic equation which remains linear also in the case of inter-particle interactions. Monte Carlo algorithms for the solution of that equation are based on the computation and sampling of trajectory pairs. Two wave vectors, $\mathbf{k}_1$ and $\mathbf{k}_2$, are considered simultaneously, which means that the method is actually sampling the six-dimensional momentum space. Doubling the dimension of momentum space, however, does not degrade the efficiency of the Monte Carlo method as it does not suffer from the curse of dimensionality, in stark contrast to deterministic methods.

2. Transport model

In the presence of a uniform electric field, the Boltzmann equation for electrons is of the form

$$\left(\frac{\partial}{\partial t}+\frac{e}{\hbar}\mathbf{E}\cdot\nabla_k\right)f(\mathbf{k},t)=Q[f](\mathbf{k},t). \tag{1}$$

This single-particle kinetic equation becomes nonlinear when EES is included in the scattering operator Q.

$$Q[f](\mathbf{k})=\int S(\mathbf{k},\mathbf{k}')f(\mathbf{k}')-S(\mathbf{k}',\mathbf{k})f(\mathbf{k}')d\mathbf{k}'. \tag{2}$$

In the case of EES, the single-particle scattering rate S will depend on the unknown distribution function f.

$$S(\mathbf{k}_1,\mathbf{k}_1')=\iint P(\mathbf{k}_1,\mathbf{k}_2,\mathbf{k}_1',\mathbf{k}_2')f(\mathbf{k}_2)d\mathbf{k}_2d\mathbf{k}_2' \tag{3}$$

Integration is over all degrees of freedom of the partner electron, i.e., its initial momentum $\mathbf{k}_2$ and final momentum $\mathbf{k}_2'$. In the case of two-particle interactions, it is advantageous to resort to a two-particle kinetic equation.

$$\begin{aligned}\left(\frac{\partial}{\partial t}+\frac{e}{\hbar}\left(\mathbf{E}\cdot\nabla_1+\mathbf{E}\cdot\nabla_2\right)\right)g(\mathbf{k}_1,\mathbf{k}_2,t)\\ =\left(Q_{\mathrm{ph}}+Q_{\mathrm{ee}}\right)[g](\mathbf{k}_1,\mathbf{k}_2,t)\end{aligned} \tag{4}$$

In this formulation, Q_{ee} is a linear operator acting on the two-particle distribution function g.

$$\begin{aligned}Q_{\mathrm{ee}}[g](\mathbf{k}_1,\mathbf{k}_2,t)=\iint P(\mathbf{k}_1,\mathbf{k}_2,\mathbf{k}_1',\mathbf{k}_2')\\ \left[g(\mathbf{k}_1',\mathbf{k}_2')-g(\mathbf{k}_1,\mathbf{k}_2,t)\right]d\mathbf{k}_1'd\mathbf{k}_2'\end{aligned}$$

Stationary and transient Monte-Carlo algorithms for the solution of (4) have been proposed in [8].

3. Scattering rates

Electron–phonon scattering in silicon is treated by the model reported in [9]. The concept of self-scattering with a constant self-scattering rate is used for efficient calculation of the free flight time.

☆ The review of this paper was arranged by Prof. Sorin Cristoloveanu.

* Corresponding author.
E-mail address: josef.gull@tuwien.ac.at (J. Gull).

https://doi.org/10.1016/j.sse.2023.108730

Available online 10 August 2023

For electron–electron scattering a screened Coulomb interaction potential U_s is assumed.

$$U_S(u) = \frac{e^2}{4\pi\epsilon_s}\frac{\exp(-u\beta_s)}{u} \tag{5}$$

The distance between two electrons is denoted by $u = |\mathbf{r}_2 - \mathbf{r}_1|$ and the inverse screening length by β_s. In order to calculate the scattering rate, the transition rate according to Fermi's golden rule has to be evaluated first. The state of an electron pair is written as a product of two plane wave states. The wavefunction of a state $|\mathbf{k}_1, \mathbf{k}_2\rangle$ reads

$$\Psi_{\mathbf{k}1,\mathbf{k}2}(\mathbf{r}_1, \mathbf{r}_2) = \frac{1}{\Omega} e^{i(\mathbf{k}_1\cdot\mathbf{r}_1 + \mathbf{k}_2\cdot\mathbf{r}_2)} \tag{6}$$

Using wavefunctions of this form, the matrix element of (5) evaluates to

$$\left\langle \mathbf{k}_1', \mathbf{k}_2' \right| U_S \left| \mathbf{k}_1, \mathbf{k}_2 \right\rangle = \left[\frac{e^2}{\epsilon_s \Omega}\right] \frac{\delta_{\mathbf{k}_1+\mathbf{k}_2, \mathbf{k}_1'+\mathbf{k}_2'}}{|\mathbf{k}_1 - \mathbf{k}_1'|^2 + \beta_s^2}. \tag{7}$$

The transition probability is then given by Fermi's golden rule.

$$P(\mathbf{k}_1, \mathbf{k}_2, \mathbf{q}) = \frac{2\pi}{\hbar}\left[\frac{e^2}{\epsilon_s\Omega}\right]^2 \times \frac{\delta[\epsilon(\mathbf{k}_1+\mathbf{q}) + \epsilon(\mathbf{k}_2-\mathbf{q}) - \epsilon(\mathbf{k}_1') - \epsilon(\mathbf{k}_2')]}{\left(|\mathbf{q}|^2 + \beta_s^2\right)^2} \tag{8}$$

The Kronecker-δ in (7) and the Dirac-δ in (8) express the fact that only such transitions are allowed which conserve total momentum and total energy of the electron pair. In the above equation, we have introduced the momentum transfer vector $\mathbf{q} = \mathbf{k}_1' - \mathbf{k}_1$. The total scattering rate Γ_{ee} is found by multiplying the transition rate (8) with the density of states and integrating over all momentum transfer vectors.

$$\Gamma_{ee}(\mathbf{k}_1, \mathbf{k}_2) = \frac{ne^4 m}{4\pi\hbar^3\epsilon_s^2\beta_s^2}\frac{K}{K^2+\beta_s^2} \tag{9}$$

In this equation, K is defined as $K = |\mathbf{K}|$ with $\mathbf{K} = \mathbf{k}_2 - \mathbf{k}_1$.

For the evaluation of the two electron states after an EES event, a random momentum transfer vector has to be generated. Integration of (8) over the polar angle ϑ, defined via $\mathbf{q}\cdot\mathbf{K} = qK\cos\vartheta$, yields the probability distribution of q.

$$p(q) = C\frac{q^2}{(q^2+\beta_s^2)^2}, \qquad 0 \le q \le K \tag{10}$$

The magnitude q is calculated using the inversion method. From two random numbers $r_1, r_2 \in [0, 1)$ the spherical coordinates of the random vector $\mathbf{q}_r$ are obtained as follows.

$$q_r^2 = \frac{r_1 K^2\beta_s^2}{K^2(1-r_1)+\beta_s^2} \tag{11a}$$

$$\cos\vartheta_r = \frac{q_r}{K}, \quad \varphi_r = 2\pi r_2. \tag{11b}$$

The new wave vectors $\mathbf{k}_1'$ and $\mathbf{k}_2'$ are given by

$$\mathbf{k}_1' = \mathbf{k}_1 + \mathbf{q}_r, \qquad \mathbf{k}_2' = \mathbf{k}_2 - \mathbf{q}_r. \tag{12}$$

4. Bulk algorithm

The stationary and transient MC algorithms are based on the computation of trajectory pairs. At each instant in time the motion of two electrons is considered. The duration of the simultaneous free flights is generated from an exponential distribution. For this purpose the self-scattering method can be used which requires the addition of a self-scattering rate Γ_{ss} to the physical scattering rate so as to obtain a constant rate $\Gamma_{\max}$. The difference $\mathbf{K} = \mathbf{k}_2(t) - \mathbf{k}_1(t)$ remains constant during a free flight, and so does the rate Γ_{ee}. Therefore, self-scattering rates have to be added only to the phonon rates Γ_{ph}.

$$\begin{aligned}\Gamma_{\max} &= \Gamma_{\mathrm{ph}}(\mathbf{k}_1) + \Gamma_{\mathrm{ss}}(\mathbf{k}_1) + \Gamma_{\mathrm{ph}}(\mathbf{k}_2) + \Gamma_{\mathrm{ss}}(\mathbf{k}_2) \\ &\quad + 2\,\Gamma_{\mathrm{ee}}(\mathbf{k}_2 - \mathbf{k}_1)\end{aligned} \tag{13}$$

Here, the rate $\Gamma_{\mathrm{ph}}(\mathbf{k}) + \Gamma_{\mathrm{ss}}(\mathbf{k})$ has to be a positive constant in the energy range of interest. Having set up $\Gamma_{\max}$, the free-flight time is generated from a random number r as

$$t_f = -\frac{1}{\Gamma_{\max}}\log(1-r). \tag{14}$$

At the end of a free flight, a scattering mechanism has to be selected. With probability $\Gamma_{\mathrm{ph}}(\mathbf{k}_1)/\Gamma_{\max}$ a phonon scattering event for particle 1 is selected, whereas the state of particle 2 remains unchanged. Conversely, with probability $\Gamma_{\mathrm{ph}}(\mathbf{k}_2)/\Gamma_{\max}$ a phonon scattering event for particle 2 is selected, and the state of particle 1 is not affected. With probability $2\,\Gamma_{\mathrm{ee}}/\Gamma_{\max}$, electron–electron scattering is selected. This event changes the states of both particles simultaneously. As mentioned above, the total momentum and the total energy of both particles are strictly conserved. The complementary event is the self-scattering event, leaving the states of both particles unchanged.

Stationary averages can be computed using the before-scattering method. In this case a statistical weight of $\Gamma_{\max}^{-1}$ has to be considered. If the trajectory pair is sampled at equidistant points in time, each sampling value has equal statistical weight. This latter sampling technique is also suitable for the ensemble Monte Carlo algorithm. This algorithm calculates the response of a carrier system to a spatially uniform, time-varying electric field $\mathbf{E}(t)$ by simulating an ensemble of trajectory pairs [8].

5. Device algorithm

To simulate transport in spatially varying electric fields, the bulk algorithm has been extended. For an easier understanding, we call one electron "sample electron" (SE) and the other one "partner electron" (PE). The simulation domain is decomposed into cells, each holding one PE. Whenever a SE crosses a cell boundary, one simultaneously calculates the free flight trajectories of the SE and PE in that cell. After a sequence of free-flight and scattering events one of the two electrons will reach the cell boundary. In that case, the state at the cell boundary is used to update the averages, whereby a statistical weight of $|v_\perp|^{-1}$, i.e., the reciprocal of the normal component of the velocity, has to be used. In the next cell, a new pair of trajectories with the local field is calculated. If the PE leaves before the SE, the electrons swap their roles as PE and SE. The swap ensures that every cell always holds one PE and that the algorithm treats both electrons equally. This algorithm is restricted to time-independent field distributions since it relies on the time-invariance of the trajectories. The free flight of one electron is interrupted when the other reaches a cell boundary and will be continued at a later point in time when another SE enters that cell. In the special case of non-interacting particles, which can be used as a test case, this two-particle algorithm reproduces exactly the results of the single-particle algorithm.

6. Results

Numerical results were obtained for a single-valley band structure model assuming the material parameters of silicon [9]. Fig. 1 shows that EES has no visible effect on the distribution function in a bulk semiconductor. This is consistent with the observation, that the field-dependences of mean values such as mean velocity and mean energy are also not altered by EES. This is remarkable since EES is a dominant mechanism, and in many situations EES occurs more frequently than phonon scattering.

For the device simulations, an analytical potential profile has been assumed. The electric field is zero in the contacts, whereas in the channel of length 50 nm it varies quadratically. In the simulation of

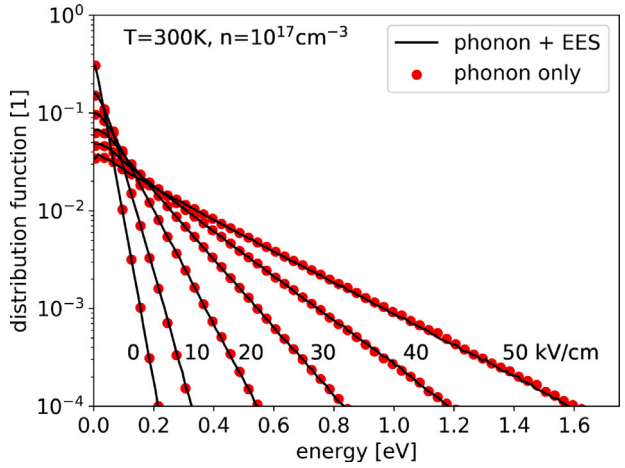

Fig. 1. Distribution functions in bulk for different field strengths, calculated with and without EES. EES has no visible influence.

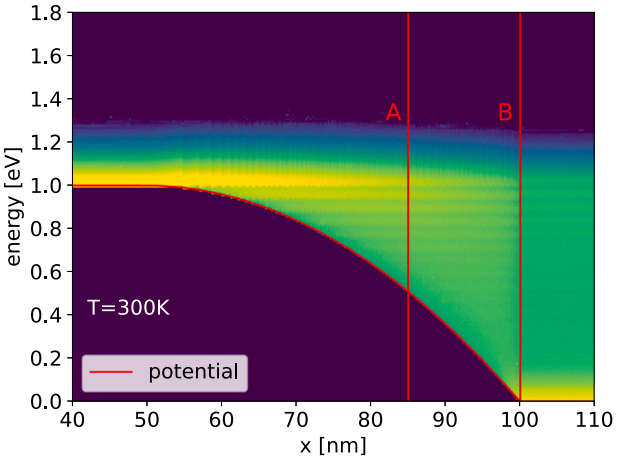

Fig. 2. Energy distribution in a channel calculated without EES. The wavelike pattern has the period of the dominant phonon energy. At positions A and B the potential drop amounts to 0.5 eV and 1 eV, respectively.

the EDF shown in Fig. 2, only phonon scattering was considered. The dominant phonon energy gives the period of the wavelike pattern. Whenever the potential drops below n times the phonon energy, a new period of the pattern begins. The effect is much weaker when EES is included (Fig. 3). We also analyzed EDFs at certain positions in the channel where the potential dropped below specific energies (at point A the potential drop is 0.5 eV, at point B 1 eV). In Fig. 4, the oscillations at positions A and B are clearly visible. In Figs. 5 and 6, the influence of the electron density can be seen at points A and B, respectively. EES causes a deviation from the thermal tail, which is obtained if only phonon scattering is assumed. For higher carrier concentrations, many more high-energetic electrons are obtained.

7. Conclusion and outlook

We showed that EES plays an important role in the calculation of the EDF. Results from [2] regarding the enhancement in the high-energy tail have been qualitatively reproduced. For a better resolution of the high-energy part of the EDF, we currently work on statistical enhancement methods such as the particle splitting/gathering method.

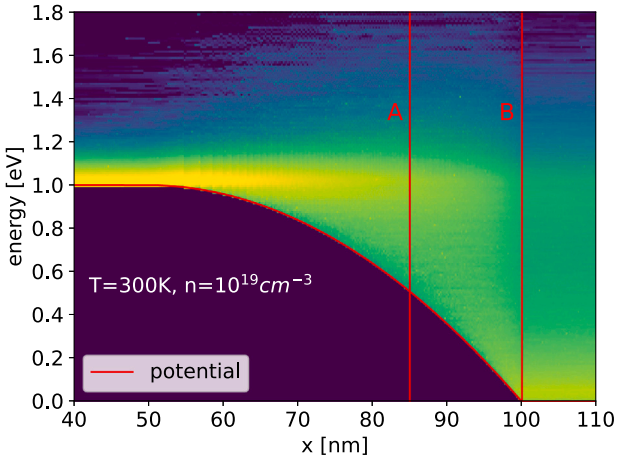

Fig. 3. Energy distribution when phonon scattering and EES are included. The additional EES suppresses the wavelike pattern.

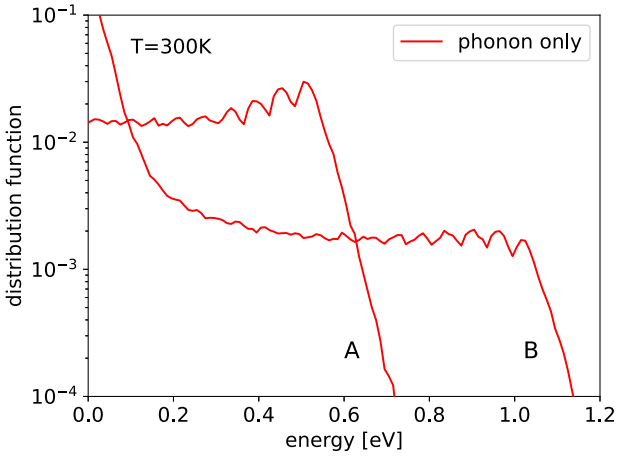

Fig. 4. Oscillations in the EDF at position A and B calculated without EES. The thermal tails are separated by 0.5 eV.

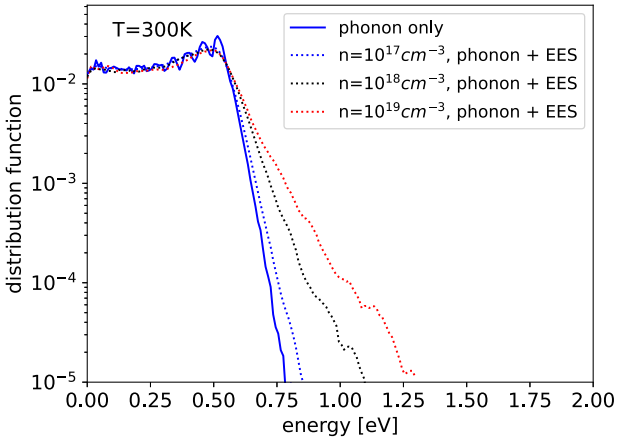

Fig. 5. Distribution functions at position A with and without EES at three different carrier densities.

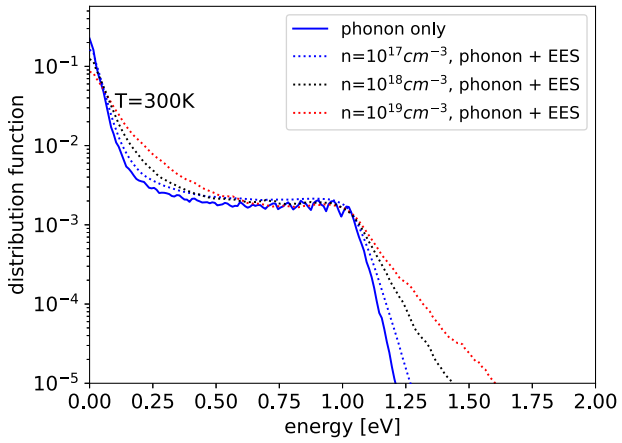

Fig. 6. Distribution functions at position *B* with and without EES at three different carrier densities.

Declaration of competing interest

The authors declare that they have no known competing financial interests or personal relationships that could have appeared to influence the work reported in this paper.

Data availability

The authors are unable or have chosen not to specify which data has been used.

Acknowledgment

This work has been supported by the Austrian Research Promotion Agency (FFG), contract 880672. The authors acknowledge TU Wien Bibliothek for financial support through its Open Access Funding Programme.

References

[1] Grasser T. Hot carrier degradation in semiconductor devices. Springer; 2014.
[2] Childs PA, Leung CCC. J Appl Phys 1996;79(1):222–7. http://dx.doi.org/10.1063/1.360935.
[3] Mietzner T, Jakumeit J, Ravaioli U. VLSI Des 2001;13(1–4):175–8.
[4] Reaz M, Tonigan AM, Li K, Smith MB, Rony MW, Gorchichko M, O'Hara A, Linten D, Mitard J, Fang J, et al. IEEE Trans Electron Devices 2021;68(5):2556–63.
[5] Brunetti R, Jacoboni C, Matulionis A, Dienys V. Physica B+C 1985;134(1):369–73. http://dx.doi.org/10.1016/0378-4363(85)90373-0.
[6] Artaki M, Hess K. Phys Rev B 1988;37:2933–45. http://dx.doi.org/10.1103/PhysRevB.37.2933.
[7] Goodnick SM, Lugli P. Phys Rev B 1988;37:2578–88.
[8] Gull J. Implementation of a two-particle Monte Carlo method for the treatment of electron-electron scattering in semiconductors (Master's thesis), Vienna, AUT: Technical University of Vienna; 2022.
[9] Jacoboni C, Lugli P. The Monte Carlo method for semiconductor device simulation. Springer Science & Business Media; 2012.